Controller Mode and Reference Governor for Constraint and Failure Management in Vehicle Platoon Systems

Ran Tian, Nan Li, Anouck Girard, and Ilya Kolmanovsky

***Abstract*— Platooning has a potential to improve traffic efficiency and fuel economy by allowing vehicles to travel with shorter inter-vehicle distances. However, shorter distances require stricter safety management, including degradation and failure mode effects management. This paper proposes a controller mode and reference governor (CMRG) scheme for constraint and failure management in vehicle platoon systems. The CMRG is an add-on supervisor for multi-mode controlled systems that monitors and adjusts the control modes and reference inputs to enforce constraints. Through simulations we show that with CMRG, safety constraints can be enforced and sensor and/or actuator degradations/failures can be managed in vehicle platoon systems.**

I. Introduction

A vehicle platoon is a string of vehicles traveling together with a harmonized speed and pre-specified inter-vehicle distances [1]. Platooning has been shown to be an effective way to improve traffic efficiency and fuel economy [2], [3]. Various challenges of vehicle platoon systems, including platoon formation [4], [5], string stability [6]–[8], heterogeneity [9], [10], interaction topology [11], [12] and delay effects [13], [14] have been addressed. The benefits of platooning are mainly attributed to shorter inter-vehicle distances, which can increase road capacity and reduce air resistance for the follower vehicles, thus improving their fuel economy [2]. Because the vehicles are traveling at shorter inter-vehicle distances, safety, in terms of not having collisions, is a major concern.

Many safety requirements, including collision avoidance, can be imposed as constraints. Reference governors are add-on, supervisory schemes for closed-loop systems that handle constraints by monitoring and adjusting the commands/reference inputs to the system [15]. In this paper, we consider an extension of the reference governor scheme, referred to as *Controller Mode and Reference Governor* (CMRG), which manipulates both the control modes of and the reference inputs to the system to enforce constraints and mitigate degradation/failure effects when they occur. Although a reference governor for multi-mode controlled systems has been proposed in [16], the use for failure mode effects management (FMEM) has not been considered. Furthermore, we use the proposed CMRG to enforce probabilistic chance constraints in vehicle platoon systems subject to stochastic disturbances, and to handle their sensor and/or actuator degradations/failures.

This research was supported by the National Science Foundation Award ECCS 1931738.

R. Tian, N. Li, A. Girard, and I. Kolmanovsky are with the Department of Aerospace Engineering, University of Michigan, Ann Arbor, MI 48109, USA. {tianran, nanli, anouck, ilya}@umich.edu.

II. Multi-Mode Controlled System

In this paper, we consider systems represented by the following discrete-time model,

$$x(k+1) = Ax(k) + B_u u(k) + B_w w(k), \tag{1a}$$
$$y(k) = Cx(k) + D_u u(k) + D_w w(k), \tag{1b}$$

where $x(k) \in \mathbb{R}^{n_x}$ represents the system state at the discrete time instant $k \in \mathbb{Z}_{\geq 0}$, $u(k) \in \mathbb{R}^{n_u}$ represents the control input, $w(k) \in \mathbb{R}^{n_w}$ represents the disturbance input, and $y(k) \in \mathbb{R}^{n_y}$ represents the system output. We assume that the disturbance input $w(k)$ takes values randomly according to a normal distribution with mean 0 and covariance W, denoted as $w(k) \sim \mathcal{N}(0, W)$, and independently for each $k \in \mathbb{Z}_{\geq 0}$.

We assume that a finite set of control policies has been defined to stabilize the system to desired steady states. They have the following form,

$$u(k) = F^j \hat{x}(k) + G^j v(k), \quad j = 0, 1, ..., n_m, \tag{2}$$

where $\hat{x}(k)$ represents a measurement/estimate of the system state $x(k)$, and $v(k) \in \mathbb{R}^{n_v}$ represents the reference input which determines the desired steady state of the system. In particular, we assume $\hat{x}(k) = x(k) + \tilde{x}(k)$, where $\tilde{x}(k) \sim \mathcal{N}(0, \Sigma_0)$ is a normally-distributed measurement/estimate error. Such an error may be the outcome of a state observer (e.g., a Kalman filter). Substituting (2) into (1), we obtain

$$x(k+1) = \bar{A}^j x(k) + \bar{B}^j v(k) + w_x^j(k), \tag{3a}$$
$$y(k) = \bar{C}^j x(k) + \bar{D}^j v(k) + w_y^j(k), \tag{3b}$$

where $\bar{A}^j = A + B_u F^j$, $\bar{B}^j = B_u G^j$, $\bar{C}^j = C + D_u F^j$, $\bar{D}^j = D_u G^j$, and $w_x^j \sim \mathcal{N}(0, W_x^j)$, $w_y^j \sim \mathcal{N}(0, W_y^j)$ with $W_x^j = B_u F^j \Sigma_0 (B_u F^j)^\top + B_w W B_w^\top$, $W_y^j = D_u F^j \Sigma_0 (D_u F^j)^\top + D_w W D_w^\top$. The variable $j \in \{0, 1, ..., n_m\}$ in (2) indicates the *control mode* of the system, which can be adjusted to address constraints and sensor/actuator degradations. The following assumptions are made: 1) the matrices $\bar{A}^j$ are Schur, and 2) $\bar{C}^j (I_{n_x} - \bar{A}^j)^{-1} \bar{B}^j + \bar{D}^j$ are identical for all $j = 0, 1, ..., n_m$, meaning that for a given constant reference input $v(k) \in \mathbb{R}^{n_v}$ the steady-state outputs of different control modes are the same.

III. Constraints and Failures

A. Constraints

Constraints may be imposed on system states/outputs to represent safety requirements such as collision avoidance, or be imposed on control inputs to represent, e.g., actuator limits. We consider constraints that are expressed as

$$y(k) \in \mathcal{Y} = \left\{ y \in \mathbb{R}^{n_y} : y \leq y_{\text{limit}} \right\}. \tag{4}$$

Note that (4) can represent both state/output and input constraints by properly choosing the matrix pair (C, D_u). For systems modeled as (1) with stochastic inputs, it is

typical to enforce the constraint (4) probabilistically as $\mathbb{P}\big(y(k) \in \mathcal{Y}\big) \geq \gamma$ [17], [18]. On the one hand, it is in general not possible to enforce (4) deterministically due to the presence of the Gaussian noise $w(k) \sim \mathcal{N}(0, W)$ and $\tilde{x}(k) \sim \mathcal{N}(0, \Sigma_0)$, which can take arbitrarily large values with positive probabilities. On the other hand, the parameter $\gamma \in (0, 1)$, representing a probabilistic guarantee for constraint enforcement, can be used as a tuning parameter to balance the tradeoff between performance and robustness, reducing the conservativeness of the design.

B. Degradations and failures

In addition to constraints, the management of degradations and failures is another important task, especially for safety critical systems. Two typical types of failures for control systems are sensor failures and actuator failures.

We model a sensor degradation/failure as a change in the measurement covariance Σ_0. In particular, we consider

$$\tilde{x}(k) \sim \mathcal{N}(0, \Sigma_0^p), \tag{5}$$

where the set of positive semi-definite matrices Σ_0^p, $p = 0, ..., n_p$, represents the measurement covariance for normal case ($p = 0$) and for pre-specified different degradation/failure cases ($p = 1, ..., n_p$). We remark that modeling a sensor failure as a change of Σ_0 is reasonable, as in many safety critical applications the state measurement $\hat{x}(k)$ used in the control law (2) is obtained by fusing the measurements of multiple, and at times redundant, sensors to reduce the measurement covariance. Then, a failure in one or more of the sensors typically results in an increase in the measurement covariance.

An actuator degradation/failure often causes its capability of providing force or power to decrease, or in other words, causes its limits to change. Since input constraints representing such limits can be incorporated in (4), we model an actuator degradation/failure by considering

$$y(k) \in \mathcal{Y}^q = \big\{y \in \mathbb{R}^{n_y} : y \leq y^q_{\text{limit}}\big\}, \tag{6}$$

where the set of output limits y^q_{limit}, $q = 0, ..., n_q$, represents the constraints (including the actuator limits) for normal case ($q = 0$) and for pre-specified different failure cases ($q = 1, ..., n_q$). We also remark that failures in many other subsystems are often handled by limited operating strategy, which restricts the actuator authority (e.g., limp home throttle position, transmission locked in third gear, etc). Such failures can also be represented as changed control input constraints.

IV. Controller Mode and Reference Governor

The CMRG is a supervisor that manages the control mode $j = 0, 1, ..., n_m$ and the reference input $v(k) \in \mathbb{R}^{n_v}$ according to current system status (normal or failure) to enforce constraints. It operates based on a collection of output admissible sets defined as follows:

$$\begin{aligned}\mathcal{O}_N(j, p, q) = \big\{(x_0, v) :\ &\text{If } x(0) \sim \mathcal{N}(x_0, \Sigma_0^p), v(k) \equiv v,\\ &\text{then } \mathbb{P}\big(y^j(k) \in \mathcal{Y}^q\big) \geq \gamma \text{ for } k = 0, 1, ..., N\big\},\end{aligned} \tag{7}$$

where $y^j(k)$ is the output of the system (3) corresponding to the control mode j, and $N \in \mathbb{N} \cup \{\infty\}$ is a specified planning horizon. Because the exact construction of $\mathcal{O}_N(j, p, q)$ requires evaluation of $\mathbb{P}\big(y^j(k) \in \mathcal{Y}^q\big)$, which involves integration of the density function of a multivariate normal distribution over a polyhedral set and is in general computationally difficult [19], we consider the following subset of $\mathcal{O}_N(j, p, q)$,

$$\begin{aligned}\tilde{\mathcal{O}}_N(j, p, q) = \big\{(x_0, v) :\ &\text{If } \hat{x}(0) = x_0, v(k) \equiv v,\\ &\text{then } \hat{y}^j(k) \in \mathcal{Y}^q \sim \mathcal{P}^{j,p}(k) \text{ for } k = 0, 1, ..., N\big\},\end{aligned} \tag{8}$$

where $\hat{y}^j(k)$ is the output of the disturbance-free system

$$\begin{aligned}\hat{x}(k+1) &= \bar{A}^j \hat{x}(k) + \bar{B}^j v(k),\\ \hat{y}(k) &= \bar{C}^j \hat{x}(k) + \bar{D}^j v(k),\end{aligned} \tag{9}$$

and $\mathcal{Y}^q \sim \mathcal{P}^{j,p}(k) = \big\{y : y + \tilde{y} \in \mathcal{Y}^q \text{ for all } \tilde{y} \in \mathcal{P}^{j,p}(k)\big\}$ denotes the P(ontryagin)-difference between the sets $\mathcal{Y}^q$ and $\mathcal{P}^{j,p}(k) = \big\{y : y^\top (\Upsilon^{j,p}(k))^{-1} y \leq F^{-1}(\gamma, n_y)\big\}$. Here, $\mathcal{P}^{j,p}(k)$ is the γ-level confidence ellipsoid, $\Upsilon^{j,p}(k)$ is the output of the following system

$$\begin{aligned}\Xi(k+1) &= \bar{A}^j\, \Xi(k)\, (\bar{A}^j)^\top + B_u F^j \Sigma_0^p (B_u F^j)^\top + B_w W B_w^\top,\\ \Upsilon(k) &= \bar{C}^j\, \Xi(k)\, (\bar{C}^j)^\top + D_u F^j \Sigma_0^p (D_u F^j)^\top + D_w W D_w^\top,\end{aligned} \tag{10}$$

with the initial condition $\Xi(0) = \Xi_0^p$, and $F^{-1}(\gamma, n_y)$ is the inverse of the cumulative distribution function of the χ^2 distribution with n_y degrees of freedom evaluated at γ.

We remark that for the polyhedral set $\mathcal{Y}^q$ defined in (6), $\mathcal{Y}^q \sim \mathcal{P}^{j,p}(k)$ can be computed as [20]

$$\begin{aligned}&\mathcal{Y}^q \sim \mathcal{P}^{j,p}(k) =\\ &\Big\{y : y_i \leq \big(y^q_{\text{limit}}\big)_i - \sqrt{F^{-1}(\gamma, n_y)\big(\Upsilon^{j,p}(k)\big)_{ii}},\ i = 1, ..., n_y\Big\}.\end{aligned} \tag{11}$$

It can be seen from (9)-(11) that the set $\tilde{\mathcal{O}}_N(j, p, q)$ is characterized by a set of linear inequalities acting on the pair (x_0, v). The numerical procedure to construct $\tilde{\mathcal{O}}_N(j, p, q)$ is similar to the one in Section 3.2 of [18], and is omitted here.

Algorithm 1: CMRG

Input Current sensor-actuator status $\big(p(k), q(k)\big)$, state measurement $\hat{x}(k)$, and original reference $\hat{v}(k)$.
Output Current control mode $j(k)$ and adjusted reference $v(k)$.
Function $\big(j(k), v(k)\big) = \text{CMRG}\big(p(k), q(k), \hat{x}(k), \hat{v}(k)\big)$
Solve: $\min_{v^0} \|v^0 - \hat{v}(k)\|_S^2$ subject to $(\hat{x}(k), v^0) \in \tilde{\mathcal{O}}_N\big(0, p(k), q(k)\big)$;
if *solution exists* **then**
  return $(0, v^0)$.
else
  $V \leftarrow \emptyset$;
  for $j = 1, 2, ..., n_m$ **do**
    Solve: $\min_{v^j} \|v^j - \hat{v}(k)\|_S^2$ subject to $(\hat{x}(k), v^j) \in \tilde{\mathcal{O}}_N\big(j, p(k), q(k)\big)$;
    If solution exists, then $V \leftarrow V \cup \{v^j\}$;
  end for
  Find $v^{j^*} = \arg\min_{v^j \in V} \|v^j - \hat{v}(k)\|_S^2$ and **return** (j^*, v^{j^*}).
end if

The CMRG operates based on Algorithm 1. In Algorithm 1, $\hat{v}(k)$ denotes the original reference input at time k, which may represent the maneuver command from a human operator or be generated by a higher-level planning algorithm without accounting for constraints or failures, and $\|\cdot\|_S = \sqrt{(\cdot)^\top S(\cdot)}$ with S being a positive definite matrix.

After the control mode and reference pair $(j(k), v(k))$ is determined by CMRG, the system is switched to the mode $j = j(k)$ and applies the reference input $v(k)$ for one step.

When CMRG cannot find a feasible pair $(j(k), v(k))$ after searching over all available control modes $j = 0, 1, ..., n_m$ (which may result from the occurrence of a very large disturbance input realization), as a fail-safe, CMRG relaxes the constraint y^q_{limit} to $y^q_{\text{limit}} + \lambda$ with $\lambda \geq 0$ as an optimization variable representing the degree of constraint violation. Correspondingly, the constraint $(\hat{x}(k), v^j) \in \tilde{\mathcal{O}}_N\big(j, p(k), q(k)\big)$ is relaxed by replacing each of the inequality (11) with

$$y_i \leq \big(y^q_{\text{limit}}\big)_i + \lambda - \sqrt{F^{-1}(\gamma, n_y)\big(\Upsilon^{j,p}(k)\big)_{ii}}. \tag{12}$$

After that, CMRG solves for the pair (j^*, v^{j^*}) with the minimum violation λ. Theoretical properties of the CMRG Algorithm 1 could be characterized following similar steps as in [18]. This will be pursued in our future work.

V. Constraint and Failure Management in Vehicle Platoon Systems

We apply the proposed CMRG scheme to constraint and failure management in vehicle platoon systems (see Fig. 1). We first introduce the model to represent the longitudinal dynamics of a vehicle platoon and the control law to realize car-following behavior. We then introduce the models that represent constraints and sensor/actuator failures. After that, we discuss the incorporation of these models into the CMRG scheme to achieve constraint and failure management.

A. Car-following dynamics and control

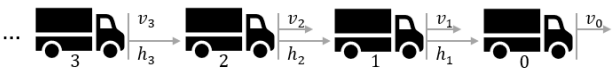

Fig. 1. Vehicle platooning illustration.

In a vehicle platoon, each vehicle $i = 1, ..., n_v$ follows its preceding vehicle $i-1$ according to the following dynamics

$$\dot{h}_i(t) = v_{i-1}(t) - v_i(t), \tag{13a}$$
$$\dot{v}_i(t) = u_i(t), \tag{13b}$$

where h_i denotes vehicle i's headway distance to vehicle $i-1$, v_i denotes vehicle i's longitudinal speed, and u_i denotes its longitudinal acceleration and is the controlled signal.

We consider the following controller for u_i,

$$u_i(t) = \hat{u}_i(k\Delta t), \tag{14}$$

for $t \in [k\Delta t, (k+1)\Delta t)$, where

$$\hat{u}_i(t) = \alpha_i\big(\hat{h}_i(t) - h_i^r(t)\big) + \beta_i\big(\hat{v}_{i-1}(t) - v_i(t)\big), \tag{15}$$

in which $\hat{h}_i$ is a measurement of the headway distance h_i, $\hat{v}_{i-1}$ is a measurement of the preceding vehicle's speed v_{i-1}, the gain α_i is used to match the measured headway distance $\hat{h}_i$ to a reference headway distance h_i^r, and the gain β_i is used to match the ego vehicle's speed v_i to the measured speed of the preceding vehicle $\hat{v}_{i-1}$. We assume $\hat{h}_i(t) = h_i(t) + \tilde{h}_i(t)$ and $\hat{v}_{i-1}(t) = v_{i-1}(t) + \tilde{v}_{i-1}(t)$, where $\tilde{h}_i(t) \sim \mathcal{N}(0, w_i^h)$ and $\tilde{v}_{i-1}(t) \sim \mathcal{N}(0, w_i^v)$ are normally distributed measurement errors. We also assume each vehicle i can measure its own speed $v_i(t)$ perfectly. Note that the piecewise constant control signal (14) accounts for the fact that measurements are taken at sample time instants $t = k\Delta t$, $k \in \mathbb{Z}_{\geq 0}$.

Substituting (14) and (15) into (13), we obtain

$$\dot{h}_i(t) = v_{i-1}(t) - v_i(t), \tag{16a}$$
$$\dot{v}_i(t) = \alpha_i\big(h_i(k\Delta t) - h_i^r(k\Delta t)\big) + \beta_i\big(v_{i-1}(k\Delta t) - v_i(k\Delta t)\big) + \alpha_i\tilde{h}_i(k\Delta t) + \beta_i\tilde{v}_{i-1}(k\Delta t), \tag{16b}$$

for $t \in [k\Delta t, (k+1)\Delta t)$, $k \in \mathbb{Z}_{\geq 0}$.

Assuming $v_{i-1}(t)$ stays constant over $[k\Delta t, (k+1)\Delta t)$ and integrating (16), we further obtain

$$h_i(k+1) = \big(1 - \frac{\Delta t^2}{2}\alpha_i\big)h_i(k) - \big(\Delta t - \frac{\Delta t^2}{2}\beta_i\big)v_i(k) + \frac{\Delta t^2}{2}\alpha_i h_i^r(k) + \big(\Delta t - \frac{\Delta t^2}{2}\beta_i\big)v_{i-1}(k) - \frac{\Delta t^2}{2}\big(\alpha_i\tilde{h}_i(k) + \beta_i\tilde{v}_{i-1}(k)\big), \tag{17a}$$

$$v_i(k+1) = \Delta t\,\alpha_i h_i(k) + (1 - \Delta t\,\beta_i)v_i(k) - \Delta t\,\alpha_i h_i^r(k) + \Delta t\,\beta_i v_{i-1}(k) + \Delta t\big(\alpha_i\tilde{h}_i(k) + \beta_i\tilde{v}_{i-1}(k)\big). \tag{17b}$$

Note that k and $k+1$ in the above expressions correspond to the discrete time instants $k\Delta t$ and $(k+1)\Delta t$. In matrix form, the discrete-time dynamics (17) can be written as

$$x_i(k+1) = A_i x_i(k) + B_i h_i^r(k) + \Phi_i v_{i-1}(k) + \Psi_i w_i(k), \tag{18}$$

where $x_i(k) = \big[h_i(k),\, v_i(k)\big]^\top$, $w_i(k) = \big[\tilde{h}_i(k),\, \tilde{v}_{i-1}(k)\big]^\top$,

$$A_i = \begin{bmatrix} 1 - \frac{\Delta t^2}{2}\alpha_i & -\Delta t + \frac{\Delta t^2}{2}\beta_i \\ \Delta t\,\alpha_i & 1 - \Delta t\,\beta_i \end{bmatrix}, \quad B_i = \begin{bmatrix} \frac{\Delta t^2}{2}\alpha_i \\ -\Delta t\,\alpha_i \end{bmatrix},$$
$$\Phi_i = \begin{bmatrix} \Delta t - \frac{\Delta t^2}{2}\beta_i \\ \Delta t\,\beta_i \end{bmatrix}, \quad \Psi_i = \begin{bmatrix} -\frac{\Delta t^2}{2}\alpha_i & -\frac{\Delta t^2}{2}\beta_i \\ \Delta t\,\alpha_i & \Delta t\,\beta_i \end{bmatrix}. \tag{19}$$

The reference headway distance h_i^r, which determines the steady-state car-following distance as $h_i^* = h_i^r$, is a design variable. It is often designed as a function of the preceding vehicle's speed, i.e., $h_i^r(k) = G\big(v_{i-1}(k)\big)$, called a *range policy*. We consider the following range policy, which is modified from the range policies proposed in [10], [21],

$$h_i^r(k) = G\big(v_{i-1}(k)\big) = \begin{cases} h_{\text{lo}} & 0 \leq v_{i-1}(k) \leq v_{\text{lo}}, \\ h_{\text{lo}} + \frac{v_{i-1}(k) - v_{\text{lo}}}{v_{\text{up}} - v_{\text{lo}}}(h_{\text{up}} - h_{\text{lo}}) & v_{\text{lo}} \leq v_{i-1}(k) \leq v_{\text{up}}, \\ h_{\text{up}} & v_{i-1}(k) \geq v_{\text{up}}. \end{cases} \tag{20}$$

B. Car-following constraints

Two types of constraints are considered in this paper. The first type is imposed on the headway distance $h_i(k)$. On the one hand, $h_i(k)$ should not be too small to avoid rear-end collisions; on the other hand, $h_i(k)$ should not be too large to prevent other cars from cutting in. Specifically, we consider the following constraints on $h_i(k)$,

$$h_{\min} \leq h_i(k) \leq h_{\max}. \tag{21}$$

The second type of constraints represents actuator limits. In particular, we consider the following constraints on $u_i(k)$,

$$a_{\min} \leq u_i(k) = \alpha_i\big(h_i(k) + \tilde{h}_i(k) - h_i^r(k)\big) + \beta_i\big(v_{i-1}(k) + \tilde{v}_{i-1}(k) - v_i(k)\big) \leq a_{\max}. \tag{22}$$

For instance, the upper bound $a_{\max} > 0$ may represent an engine power limit and the lower bound $a_{\min} < 0$ may represent a braking force limit. In matrix form, the constraints (21) and (22) can be written as

$$\begin{bmatrix} h_{\min} \\ a_{\min} \end{bmatrix} \leq y_i(k) \leq \begin{bmatrix} h_{\max} \\ a_{\max} \end{bmatrix}, \tag{23}$$

where

$$y_i(k) = C_i x_i(k) + D_i h_i^r(k) + \Theta_i v_{i-1}(k) + \Xi_i w_i(k), \tag{24}$$

$$C_i = \begin{bmatrix} 1 & 0 \\ \alpha_i & -\beta_i \end{bmatrix}, D_i = \begin{bmatrix} 0 \\ -\alpha_i \end{bmatrix}, \Theta_i = \begin{bmatrix} 0 \\ \beta_i \end{bmatrix}, \Xi_i = \begin{bmatrix} 0 & 0 \\ \alpha_i & \beta_i \end{bmatrix}.$$

Due to the presence of the Gaussian noise $w_i(k) = \left[\tilde{h}_i(k),\, \tilde{v}_{i-1}(k)\right]^\top$, we enforce (23) probabilistically as,

$$\mathbb{P}\left(\begin{bmatrix} h_{\min} \\ a_{\min} \end{bmatrix} \le y_i(k) \le \begin{bmatrix} h_{\max} \\ a_{\max} \end{bmatrix} \right) \ge \gamma, \quad \gamma \in (0,1). \tag{25}$$

C. Sensor and actuator failures

1) Sensor failure: The $\hat{h}_i$ and $\hat{v}_{i-1}$ values used to compute the control (15) are usually derived by fusing the measurements of multiple sensors, such as radar, lidar and cameras, so that uncertainty can be reduced. In turn, a failure in one or more of the sensors typically results in an increase in the uncertainty. Therefore, we model a sensor failure as a change in the measurement covariance. In particular, $w_i(k) = \left[\tilde{h}_i(k) \quad \tilde{v}_{i-1}(k)\right]^\top \sim \mathcal{N}(0, W_i^p)$, where $p = 0$ corresponds to the normal measurement covariance and $p = 1, ..., n_p$ correspond to the covariances of a pre-specified set of sensor failure cases. For instance, suppose $\hat{h}_i$ and $\hat{v}_{i-1}$ are derived by fusing the radar, lidar and camera measurements. Then, depending on the state of health of each of the three sensors, there are in total 8 cases, including 1 normal case, and $n_p = 7$ failure cases.

2) Actuator failure: The bounds $a_{\max}$ and $a_{\min}$ on u_i represent engine/braking system limits. We model a degradation/failure in these systems (e.g., brake fading) as a change in the values of these bounds. In particular, $a_{\min}^q \le u_i(k) \le a_{\max}^q$, where $q = 0$ corresponds to the normal actuator limits and $q = 1, ..., n_q$ correspond to the limits of a pre-specified set of actuator failure cases.

D. Constraint and failure management using CMRG

The CMRG manages constraints relying on a predictive model of the system. Let $k = 0$ denote the current sample time instant and assume that a measurement $\hat{v}_{i-1}(0)$ of the preceding vehicle's current speed $v_{i-1}(0)$ has been obtained. We model the variations in preceding vehicle's speed over planning horizon stochastically as $v_{i-1}(k) = v_{i-1}(0) + \tilde{\tilde{v}}_{i-1}(k)$, where $\tilde{\tilde{v}}_{i-1}(k) \sim \mathcal{N}(0, w_{i-1}^{\text{pre}})$. Then, after augmenting the trivial dynamics $v_{i-1}(0) = v_{i-1}(0)$ to the model (18), (24) and incorporating multiple designs for the gains (α, β) in the control law (15) as well as possible adjustments of the reference signal $h_i^r(k)$, we obtain the following predictive model

$$\bar{x}_i(k+1) = \bar{A}_i^j \bar{x}_i(k) + \bar{B}_i^j \mu + \bar{\Psi}_i^j \bar{w}_i(k), \tag{26a}$$

$$y(k) = \bar{C}_i^j \bar{x}_i(k) + \bar{D}_i^j \mu + \bar{\Xi}_i^j \bar{w}_i(k), \tag{26b}$$

where $\bar{x}_i(k) = \left[h_i(k),\, v_{i-1}(0),\, v_i(k)\right]^\top$, $\bar{w}_i(k) = \left[\tilde{h}_i(k),\, \tilde{v}_{i-1}(k),\, \tilde{\tilde{v}}_{i-1}(k)\right]^\top$, and

$$\bar{A}_i^j = \begin{bmatrix} 1 - \frac{\Delta t^2}{2}\alpha_i^j & \Delta t - \frac{\Delta t^2}{2}\beta_i^j & -\Delta t + \frac{\Delta t^2}{2}\beta_i^j \\ 0 & 1 & 0 \\ \Delta t\, \alpha_i^j & \Delta t\, \beta_i^j & 1 - \Delta t\, \beta_i^j \end{bmatrix}, \tag{27}$$

$$\bar{B}_i^j = \begin{bmatrix} \frac{\Delta t^2}{2}\alpha_i^j \\ 0 \\ -\Delta t\, \alpha_i^j \end{bmatrix}, \bar{\Psi}_i^j = \begin{bmatrix} -\frac{\Delta t^2}{2}\alpha_i^j & -\frac{\Delta t^2}{2}\beta_i^j & \Delta t - \frac{\Delta t^2}{2}\beta_i^j \\ 0 & 0 & 0 \\ \Delta t\, \alpha_i^j & \Delta t\, \beta_i^j & \Delta t\, \beta_i^j \end{bmatrix},$$

$$\bar{C}_i^j = \begin{bmatrix} 1 & 0 & 0 \\ \alpha_i^j & \beta_i^j & -\beta_i^j \end{bmatrix}, \bar{D}_i^j = \begin{bmatrix} 0 \\ -\alpha_i^j \end{bmatrix}, \bar{\Xi}_i^j = \begin{bmatrix} 0 & 0 & 0 \\ \alpha_i^j & \beta_i^j & \beta_i^j \end{bmatrix}.$$

The first two components of the initial condition $\bar{x}_i(0) = \left[h_i(0),\, v_{i-1}(0),\, v_i(0)\right]^\top$ are not perfectly measured but can be estimated using the measurements $\hat{h}_i(0)$ and $\hat{v}_{i-1}(0)$ based on

$$\bar{x}_i(0) \sim \mathcal{N}\left(\begin{bmatrix} \hat{h}_i(0) \\ \hat{v}_{i-1}(0) \\ v_i(0) \end{bmatrix}, \begin{bmatrix} W_i^p & 0 \\ 0 & 0 \end{bmatrix} \right). \tag{28}$$

The disturbance input $\bar{w}_i(k) = \left[\tilde{h}_i(k),\, \tilde{v}_{i-1}(k),\, \tilde{\tilde{v}}_{i-1}(k)\right]^\top$ takes values based on

$$\bar{w}_i(k) \sim \mathcal{N}\left(0, \begin{bmatrix} W_i^p & 0 \\ 0 & w_{i-1}^{\text{pre}} \end{bmatrix}\right). \tag{29}$$

Furthermore, we have replaced the reference headway distance $h_i^r(k)$ in the model (18) with μ in (26), which is determined by solving the following optimization problem

$$\min_{\mu} \left(\mu - G(\hat{v}_{i-1}(0))\right)^2, \tag{30}$$

where $G(\cdot)$ is the range policy (20), subject to the model (26) and the following probabilistic constraint for $k = 0, 1, ..., N$,

$$\mathbb{P}\left(\begin{bmatrix} h_{\min} \\ a_{\min}^q \end{bmatrix} \le y_i(k) \le \begin{bmatrix} h_{\max} \\ a_{\max}^q \end{bmatrix} \right) \ge \gamma, \quad \gamma \in (0,1). \tag{31}$$

Up to this point, we have identified the model (3) in (26), the sensor failure model (5) in (28), (29) with $p = 0, 1, ..., n_p$, and the actuator failure model (6) in (31) with $q = 0, 1, ..., n_q$ for the specific vehicle platoon system. Then, we can apply the CMRG defined by Algorithm 1 to manage the constraints and failures of this vehicle platoon system.

VI. Simulation Results

A. Model and control parameters

The sampling period Δt is chosen as $0.1[s]$. We consider the following set of control gain pairs (i.e., control modes) for (15): $(\alpha_i^j, \beta_i^j) \in \{0.5,\, 1,\, 1.5,\, 2\} \times \{0.5,\, 1,\, 1.5,\, 2,\, 2.5,\, 3\}$, where $(\alpha_i^0, \beta_i^0) = (1, 3)$ is the nominal/default pair. The parameter values for the range policy (20) are $h_{\text{lo}} = 2[m]$, $h_{\text{up}} = 30[m]$, $v_{\text{lo}} = 0[m/s]$, and $v_{\text{up}} = 30[m/s]$. The constraints on the headway distance are set as $h_{\max} = 25[m]$ and $h_{\min} = 16[m]$. The normal measurement covariance is assumed to be $W_i^{\text{normal}} = \text{diag}(0.01^2, 0.02^2)$. The normal acceleration limits are assumed to be $a_{\max}^{\text{normal}} = 3[m/s^2]$ and $a_{\min}^{\text{normal}} = -3[m/s^2]$. For the CMRG design, we set the variance w_{i-1}^{pre} that accounts for the variations in the preceding vehicle's speed $v_{i-1}(k)$ over the planning horizon as $w_{i-1}^{\text{pre}} = 0.2^2$. The probabilistic constraint satisfaction parameter γ is chosen to be 0.99.

B. Sensor failure management in a two-vehicle platoon

The first example represents the scenario where a sensor failure occurs to the follower vehicle in a two-vehicle platoon. It is assumed that the leader vehicle (indexed by 0) drives with a trapezoidal speed profile v_0, which corresponds to the blue dash-dotted reference headway distance profile h_1^r in Fig. 2(a) according to the range policy $h_1^r = G(\hat{v}_0)$ in (20). We assume that at the time instant $t_f = 12.5[s]$, a failure occurs to the follower vehicle's sensor system, which increases the measurement covariance from $W_1^{\text{normal}} = \text{diag}(0.01^2, 0.02^2)$ to $W_1^{\text{degraded}} = \text{diag}(0.04^2, 0.08^2)$.

Fig. 2(a)-(c) show the time histories of the reference μ, headway distance h_1 and acceleration u_1 of the follower vehicle when there is no supervision (i.e., $j \equiv 0$ and $\mu \equiv h_1^r$), when a reference governor (RG) [18] is used to supervise μ but provides no supervision on controller mode (i.e., $j \equiv 0$), and when CMRG is used to supervise both controller mode and reference. The RG algorithm is similar to Algorithm 1, but does not search over the ancillary controller modes $j = 1, 2, ..., n_m$ for feasible solutions and switches directly to the fail-safe mode (12) after Step 7.

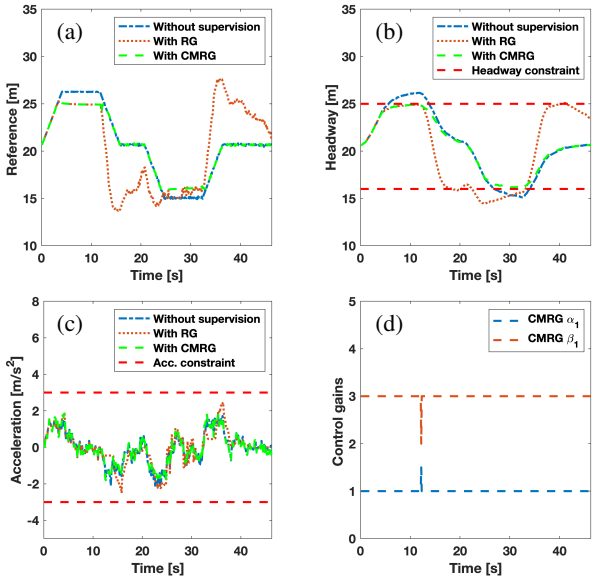

Fig. 2. Sensor failure management. (a) Original reference (blue), RG output (red), and CMRG output (green) of the follower vehicle. (b) Headway distance and (c) acceleration time histories of the follower vehicle without supervision (blue), with RG (red), and with CMRG. (d) Time history of control gains (α, β) with CMRG.

Without supervision, the headway distance constraints $h_{\max}$ and $h_{\min}$ are violated. With RG, the follower vehicle maintains its headway distance within the constrained range before the sensor failure. However, when the sensor failure occurs at $12.5[s]$, not only a large deviation of μ from h_1^r is observed but this large deviation also causes the serious failure to satisfy the headway distance lower bound $h_{\min}$ later on. This is because when the sensor failure occurs and the measurement covariance increases, the output admissible set $\tilde{\mathcal{O}}_N$ shrinks, i.e., fewer state measurement and reference input pairs are constraint admissible. When the control gains (α, β) are fixed, the RG has to significantly adjust the reference value to enforce constraints, even fails to identify a feasible solution. In contrast, with CMRG, the follower vehicle successfully maintains constraint satisfaction both before and after the sensor failure. This is because a larger set of constraint admissible state measurement and reference input pairs is achieved by issuing the follower vehicle the flexibility of choosing control gain values. The CMRG identifies the optimal pair of controller mode j and reference input μ in terms of minimizing the deviation of μ from h_1^r. Fig. 2(d) shows the time history of the control gain pair (α, β). The CMRG switches (α, β) from the default value $(1, 3)$ to $(1.5, 2)$ over a short period after the sensor failure occurs at $12.5[s]$ to enforce constraints.

Fig. 3 plots the projections of the output admissible sets $\tilde{\mathcal{O}}_N$ and trajectories of the follower vehicle on the (h_1, μ) plane. The blue and red dashed polygons in Fig. 3(a) show the $\tilde{\mathcal{O}}_N$ sets of RG before and after the sensor failure, respectively, and the dotted curve shows the vehicle trajectory under RG supervision. Before the sensor failure, the trajectory is maintained within the normal case $\tilde{\mathcal{O}}_N$ set (the blue dashed polygon). However, when the sensor failure occurs, the immediate vehicle state (highlighted by the orange point) falls outside the failure case $\tilde{\mathcal{O}}_N$ set (the red dashed polygon). This causes the failure to satisfy the headway distance constraint in Fig. 2(b). In contrast, when the sensor failure occurs, the CMRG switches the control mode to a transition mode, whose $\tilde{\mathcal{O}}_N$ set (the green dashed polygon in Fig. 3(b)) contains the immediate vehicle state. This implies the existence of a constraint admissible reference input μ, and therefore constraint satisfaction is maintained. After the trajectory enters the failure case $\tilde{\mathcal{O}}_N$ set of the default control mode (the red dashed polygon), CMRG switches the mode back to default.

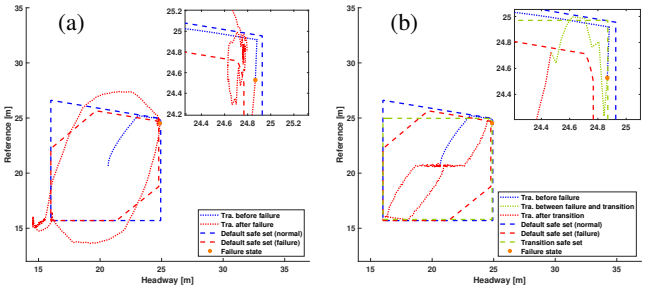

Fig. 3. Projections of output admissible sets and vehicle trajectories on the (h_1, μ) plane; (a) corresponds to RG supervision; (b) corresponds to CMRG supervision.

C. Sensor and brake failure management in two/three-vehicle platoons

We then consider the case where the sensor failure considered in the first example and a degradation/failure of the brake system occur concurrently at $t_f = 12.5[s]$ to the follower vehicle (vehicle 1). We consider such a concurrent occurrence of multiple failures to test the robustness of our CMRG design. In particular, we assume that after the brake failure occurs, the deceleration limit is decreased from $a_{\min}^{\text{normal}} = -3[m/s^2]$ to $a_{\min}^{\text{degraded}} = -1.5[m/s^2]$, illustrated by the red dashed lines in Figs. 4(c) and 5(c).

Fig. 4 shows the time histories of the reference μ_1, headway distance h_1, acceleration u_1, and control gains (α_1, β_1) of vehicle 1 without supervision, with RG, and with CMRG supervisions by blue, red, and green curves, respectively. Similar to the results of Fig. 2, without supervision, the headway distance and acceleration constraints are both violated. The RG can maintain the headway distance within the constrained range before failures, but fails to do so after failures occur. In contrast, when CMRG is used to supervise both the control mode and the reference input, the vehicle successfully maintains headway distance constraint satisfaction and violates the acceleration constraint only slightly. Note that such a slight constraint violation is due to the probabilistic enforcement of constraints (31). To

compensate for the failure effects, the CMRG switches the gain pair (α_1, β_1) from the default value $(1, 3)$ to $(0.5, 1)$ over a short period.

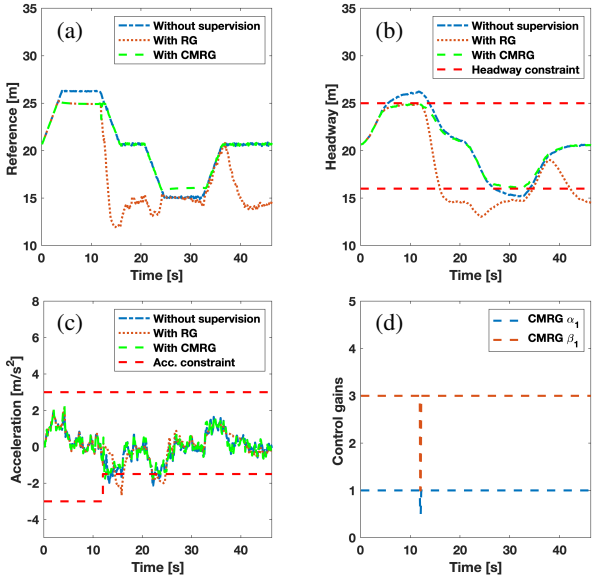

Fig. 4. Sensor and brake failure management. (a) Original reference (blue), RG output (red), and CMRG output (green) of the follower vehicle. (b) Headway distance and (c) acceleration time histories of the follower vehicle without supervision (blue), with RG (red), and with CMRG. (d) Time history of control gains (α, β) with CMRG.

Lastly, we illustrate the failure effects on the entire platoon by plotting in Fig. 5 the response of the vehicle (vehicle 2) immediately following the vehicle with sensor and actuator failures (vehicle 1). We assume that both vehicles use CMRG to supervise their control modes and reference inputs. Note that the speed profile of vehicle 1, v_1, determines the original reference headway distance profile for vehicle 2, h_2^r, according to the range policy $h_2^r = G(\hat{v}_1)$. With CMRG, vehicle 2 satisfies the headway distance constraints $h_{\min} \leq h_2 \leq h_{\max}$. Note that the deceleration limit for vehicle 2 is $a_{\min}^{\text{normal}} = -3[m/s^2]$ over the entire simulation, since vehicle 2 does not have a brake failure.

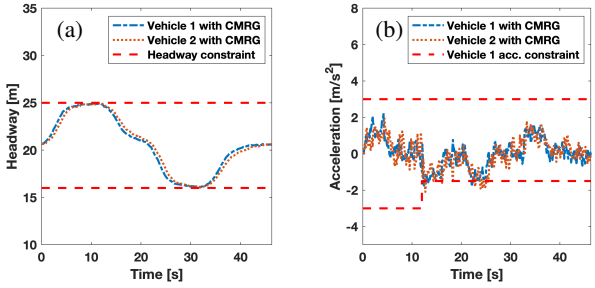

Fig. 5. Sensor and brake failure management in a three-vehicle platoon. (a) Headway distance and (b) acceleration time histories of vehicle 1 (blue) and vehicle 2 (red), where vehicle 1 has sensor and brake failures at $12.5[s]$.

VII. Conclusion

This paper considered the application of a controller mode and reference governor (CMRG) scheme to constraint and failure management in vehicle platoon systems. The CMRG monitors and adjusts the control modes and reference inputs of a multi-mode controlled system to enforce constraints and mitigate degradation/failure effects. Simulation results illustrated that with CMRG, safety constraints can be satisfactorily enforced and sensor and/or actuator degradations/failures can be managed in vehicle platoon systems.

References

[1] S. Maiti, S. Winter, and L. Kulik, "A conceptualization of vehicle platoons and platoon operations," *Transportation Research Part C: Emerging Technologies*, vol. 80, pp. 1–19, 2017.

[2] A. Alam, B. Besselink, V. Turri, J. Martensson, and K. H. Johansson, "Heavy-duty vehicle platooning for sustainable freight transportation: A cooperative method to enhance safety and efficiency," *IEEE Control Systems Magazine*, vol. 35, no. 6, pp. 34–56, 2015.

[3] C. R. He, J. I. Ge, and G. Orosz, "Fuel efficient connected cruise control for heavy-duty trucks in real traffic," *IEEE Transactions on Control Systems Technology*, pp. 1–8, 2019.

[4] F. Lin, M. Fardad, and M. R. Jovanovic, "Optimal control of vehicular formations with nearest neighbor interactions," *IEEE Transactions on Automatic Control*, vol. 57, no. 9, pp. 2203–2218, 2011.

[5] Y. Li, C. Tang, K. Li, S. Peeta, X. He, and Y. Wang, "Nonlinear finite-time consensus-based connected vehicle platoon control under fixed and switching communication topologies," *Transportation Research Part C: Emerging Technologies*, vol. 93, pp. 525–543, 2018.

[6] P. Seiler, A. Pant, and K. Hedrick, "Disturbance propagation in vehicle strings," *IEEE Transactions on Automatic Control*, vol. 49, no. 10, pp. 1835–1842, 2004.

[7] W. B. Dunbar and D. S. Caveney, "Distributed receding horizon control of vehicle platoons: Stability and string stability," *IEEE Transactions on Automatic Control*, vol. 57, no. 3, pp. 620–633, 2011.

[8] S. S. Avedisov and G. Orosz, "Analysis of connected vehicle networks using network-based perturbation techniques," *Nonlinear Dynamics*, vol. 89, no. 3, pp. 1651–1672, 2017.

[9] F. Gao, S. E. Li, Y. Zheng, and D. Kum, "Robust control of heterogeneous vehicular platoon with uncertain dynamics and communication delay," *IET Intelligent Transport Systems*, vol. 10, no. 7, pp. 503–513, 2016.

[10] N. I. Li and G. Orosz, "Dynamics of heterogeneous connected vehicle systems," *IFAC-PapersOnLine*, vol. 49, no. 10, pp. 171–176, 2016.

[11] Y. Zheng, S. E. Li, J. Wang, D. Cao, and K. Li, "Stability and scalability of homogeneous vehicular platoon: Study on the influence of information flow topologies," *IEEE Transactions on Intelligent Transportation Systems*, vol. 17, no. 1, pp. 14–26, 2015.

[12] L. Zhang and G. Orosz, "Motif-based design for connected vehicle systems in presence of heterogeneous connectivity structures and time delays," *IEEE Transactions on Intelligent Transportation Systems*, vol. 17, no. 6, pp. 1638–1651, 2016.

[13] I. G. Jin and G. Orosz, "Dynamics of connected vehicle systems with delayed acceleration feedback," *Transportation Research Part C: Emerging Technologies*, vol. 46, pp. 46–64, 2014.

[14] W. B. Qin and G. Orosz, "Scalable stability analysis on large connected vehicle systems subject to stochastic communication delays," *Transportation Research Part C: Emerging Technologies*, vol. 83, pp. 39–60, 2017.

[15] E. Garone, S. Di Cairano, and I. Kolmanovsky, "Reference and command governors for systems with constraints: A survey on theory and applications," *Automatica*, vol. 75, pp. 306–328, 2017.

[16] G. Franze, W. Lucia, and F. Tedesco, "Command governor for constrained switched systems with scheduled model transition dwell times," *International Journal of Robust and Nonlinear Control*, vol. 27, no. 18, pp. 4949–4967, 2017.

[17] A. Mesbah, "Stochastic model predictive control: An overview and perspectives for future research," *IEEE Control Systems Magazine*, vol. 36, no. 6, pp. 30–44, 2016.

[18] U. V. Kalabić, N. I. Li, C. Vermillion, and I. V. Kolmanovsky, "Reference governors for chance-constrained systems," *Automatica*, vol. 109, p. 108500, 2019.

[19] L. G. Khachiyan, "The problem of calculating the volume of a polyhedron is enumerably hard," *Russian Mathematical Surveys*, vol. 44, no. 3, p. 199, 1989.

[20] I. Kolmanovsky and E. G. Gilbert, "Theory and computation of disturbance invariant sets for discrete-time linear systems," *Mathematical Problems in Engineering*, vol. 4, no. 4, pp. 317–367, 1998.

[21] G. Orosz, "Connected cruise control: modelling, delay effects, and nonlinear behaviour," *Vehicle System Dynamics*, vol. 54, no. 8, pp. 1147–1176, 2016.